SOILS AND FOUNDATIONS Vol. 24, No. 1, 77-89, Mar. 1984
Japanese Society of Soil Mechanics and Foundation Engineering

STRESS-STRAIN CHARACTERISTICS OF SAND IN A PARTICLE-CRUSHING REGION

NORIHIKO MIURA*, HIDEKAZU MURATA** and NORIYUKI YASUFUKU***

ABSTRACT

Yield curves of sand in a particle-crushing region were determined by a multi-step stress path method under triaxial compression and extension stresses. The yield curves were found to have the characteristic $dq/dp=G(\eta)$, irrespective of the stress path, where q is the deviator stress, p, the effective mean principal stress and η, the stress ratio. Using the relationship between dq/dp and η, families of yield curves were depicted in both compression and extension stress regions. Based on a new expression for energy dissipation per unit volume, a yield curve equation was derived and this equation was proved to be well comparable with the experimental curve. An equation for predicting the stress-strain relation was also presented. This stress-strain equation was shown to be very conformable with the experimen talstress-strain curves in conditions of constant σ_r and constant p in both triaxial compression and extension stress regions.

Key words : drained shear, particle breakage (particle-crushing), sand, stress-strain curve, triaxial compression test, yield (**IGC** : D 6/E 4)

INTRODUCTION

The authors have investigated the mechanical behavior of sands in particle-crushing regions in regards to such matters as the calculation of the point resistance of piles in granular soils and the stability analysis of high fill dams. The following experimental results have been obtained (Miura et al., 1977, 1979, 1982 a).

In a high stress range, the compressibility of sand becomes so great as a result of particle-crushing that the slope of the e-ln p curve is close to that of normally consolidated clay. The threshold stress of particle-crushing is regarded as a yielding stress under a hydrostatic pressure and the stress range higher than the yielding stress is the particle-crushing region (Miura et al., 1982 a).

The effect of particle-crushing on shear strength can be understood as a decrease in a dilatancy effect caused by the particle-crush-

* Professor, Department of Construction Engineering, Faculty of Engineering, Yamaguchi University, Tokiwadai, Ube 755.
** Associate Professor, ditto.
*** Graduate Student, ditto.

Manuscript was received for review on March 2, 1983.
Written discussions on this paper should be submitted before January 1, 1985, to the Japanese Society of Soil Mechanics and Foundation Engineering, Sugayama Bldg. 4F, Kanda Awaji-cho 2-23, Chiyoda-ku, Tokyo 101, Japan.

ing, which in turn causes a decrease in the shear strength of sand. Therefore, the greater the dilatancy effect of sand is, the more the decrease in shear strength due to particle-crushing becomes.

The stress-strain curve changes considerably through particle-crushing; that is, volumetric strain increases and the peak of the stress-axial strain curve loses its sharpness. This suggests that the sand, a strain hardening-softening material in inherent (Schofield and Wroth, 1968), changes into a strain hardening material due to particle-crushing. In consideration of this, Miura (1979) pointed out that the stress-strain behavior of sand in a particle-crushing region can be predicted approximately by the Roscoe model (Roscoe and Burland, 1968) proposed for normally consolidated clay. However, there are fundamental problems in applying this model to sand in a particle-crushing region such that the predicted yield curve and stress-strain curve are considerably different from the observed data.

In order to clarify the stress-strain behavior of granular soil in particle-crushing regions, the present paper investigates the yielding characteristics of sand in detail using a multi-step stress path method under triaxial compression and extension stresses, and presents a new equation for predicting the yield curve and stress-strain curve.

SAMPLE USED

Specimen Preparation

The sand used in this study was Toyoura sand, whose main properties are as follows: specific gravity=2.64, maximum diameter=0.25mm, uniformity coefficient=1.5, maximum void ratio=0.92, and minimum void ratio=0.58.

A fully saturated specimen in a loose state (initial void ratio, about 0.84) was formed being 50mm in diameter and 130mm in height. The general procedure for the high pressure triaxial compression test was essentially the same as that of the standard triaxial test at an ordinary confining pressure. In order to perform the triaxial extension test, additional procedures were necessary in assembling the triaxial chamber. This procedure is illustrated in Fig. 1. After molding the specimen, the upper pedestal ① was joined to the piston ② by a screw ③. To avoid twisting the specimen by the screw action, the rods ④ projecting from the upper pedestal were placed in the slits of the outer cylinder ⑤.

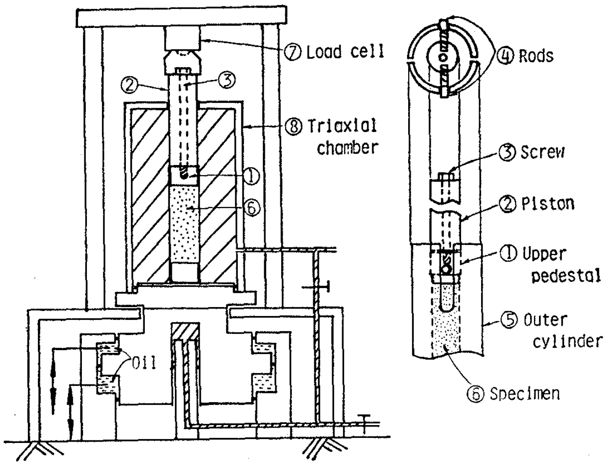

Fig. 1. Schematic diagram of high pressure triaxial apparatus

Material Constants

Three kinds of material constants, λ, κ and M, defined by Roscoe et al. (1968) were also

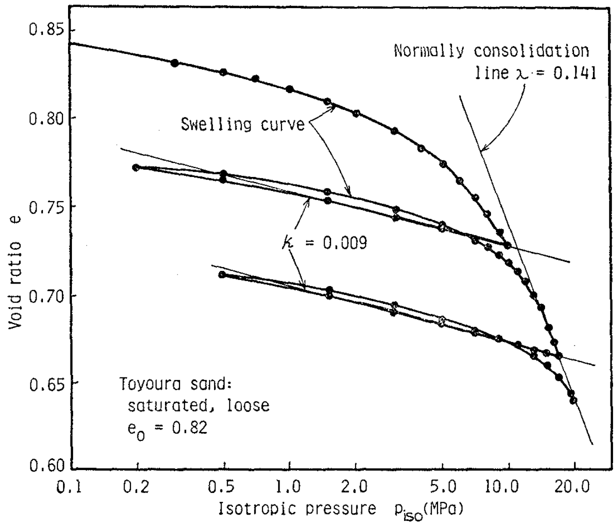

Fig. 2. Determination of soil constants λ and κ

used in this study. The constant λ is the slope of the $e-\ln p$ curve in a normally consolidated (particle-crushing) region, i.e., $\lambda=(e_1-e_2)/\ln(p_2/p_1)$, and the constant κ is the slope of the swelling curve of the $e-\ln p$ relationship as shown in Fig. 2. From these results the constants were determined as $\lambda=0.141$ and $\kappa=0.009$. Another constant M is concerned with the frictional properties of sand, and is equal to the stress ratio $\eta=q/p$ at the critical state (c.s.) (Schofield and Wroth, 1968). Let σ_a and σ_r be the axial and radial effective stresses; then,

$$\left.\begin{aligned} M&=(q/p)_{cs}=\eta_{cs}\\ q&=\sigma_a-\sigma_r\\ p&=(\sigma_a+2\sigma_r)/3 \end{aligned}\right\} \tag{2}$$

The $p-q$ plots of triaxial compression and extension tests are shown in Fig. 3, from which we obtain $M_c=1.30$ and $M_e=-0.90$. On the basis of Mohr-Coulomb hypothesis that the internal friction angle under compression stress ϕ_c is the same as that under extension stress ϕ_e, the following relationship between M_c and M_e can be derived.

$$M_e=\frac{-3M_c}{3+M_c} \tag{3}$$

Using the value $M_c=1.30$, Eq. (3) predicts that $M_e=-.091$ which is close to the observed value of -0.90.

The stress parameters p and q are associated with the strain parameters v and ε, respectively. Let ε_a and ε_r be the axial and radial principal strains, we obtain,

$$\left.\begin{aligned} \varepsilon&=\frac{2}{3}(\varepsilon_a-\varepsilon_r)\\ v&=\varepsilon_a+2\varepsilon_r \end{aligned}\right\} \tag{4}$$

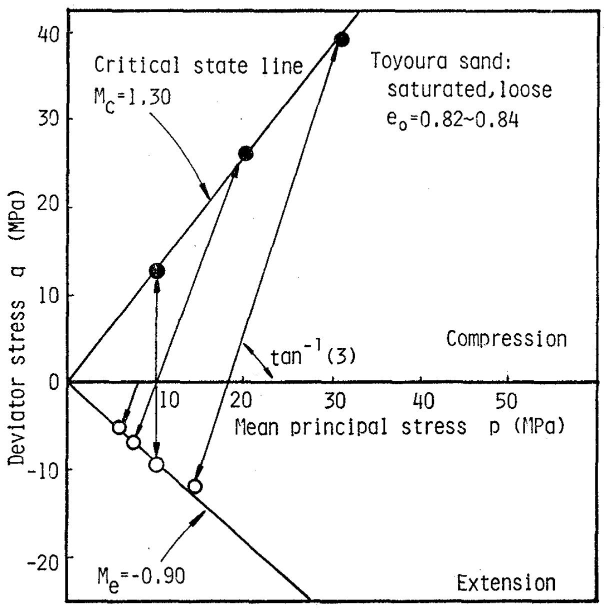

Fig. 3. p-q plot to determine the frictional constant M

MULTI-STEP STRESS PATH TEST

To investigate the characteristics of a yield curve of sand, Poorooshasb et al. (1967) and Tatsuoka et al. (1974) performed triaxial compression tests in multi-step stress paths. Referring to their methods, the authors carried out several multi-step stress path tests under both compression and extension stresses, as shown in Fig. 4 on Toyoura sand. Before shearing, each specimen was consolidated isotropically at a given pressure for about sixteen hours. For the isotropic consolidation in a specimen employed in the extension tests, the axial load P was sustained so as to yield $P=A\sigma_r$, where A is a current cross-sectional area of the specimen. The specimen was then subjected to loading and unloading according to a specified program. A single cycle of loading and unloading required about two hours. The loading was carried out in four to five steps by applying an incremental load whenever the strain rate under the present load became less than 0.01%/min (axial defor-

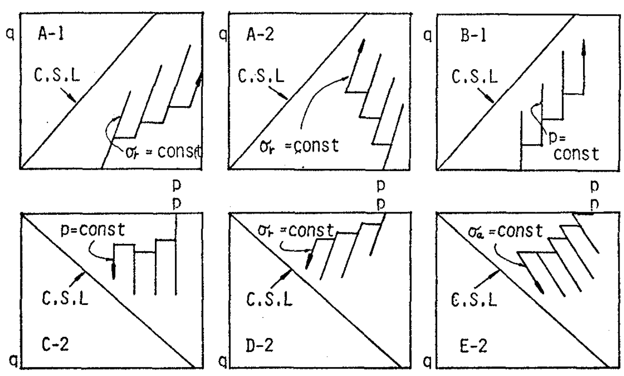

Fig. 4. Stress path for the multi-step stress path test

mation of 0.015mm per minute).

Yield points were determined on the stress-strain curves $q-\varepsilon$ and $p-v$, which are usually hyperbolic in shape (Kondner et al., 1963). While there is no generally accepted method of determining a yield point, we considered the point of maximum curvature as the yield point, in the same manner as in the previous study (Miura and Yamamoto, 1982 a).

CHARACTERISTICS OF YIELD CURVE

Yield Curve Segment

To determine the yield curve segments, Miura et al. (1982 a) employed the method illustrated in Fig. 5, in which points 1 and Y are considered to be the associated yield points. Fig. 6 indicates the family of yield curve segments determined by the above stated method, in which the segments of solid line and broken line were depicted,

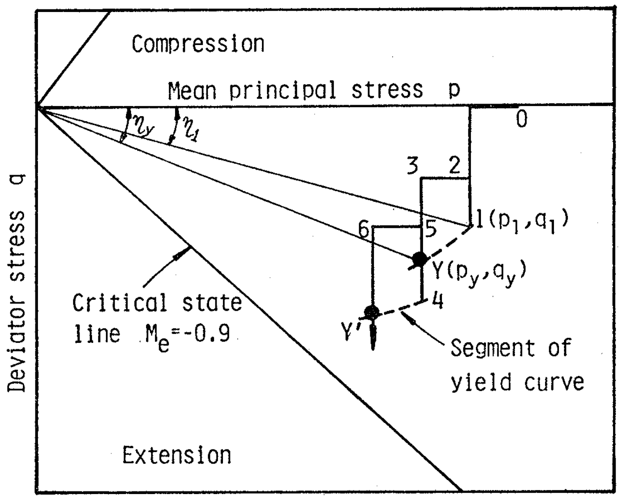

Fig. 5. Determination of segments of yield curves

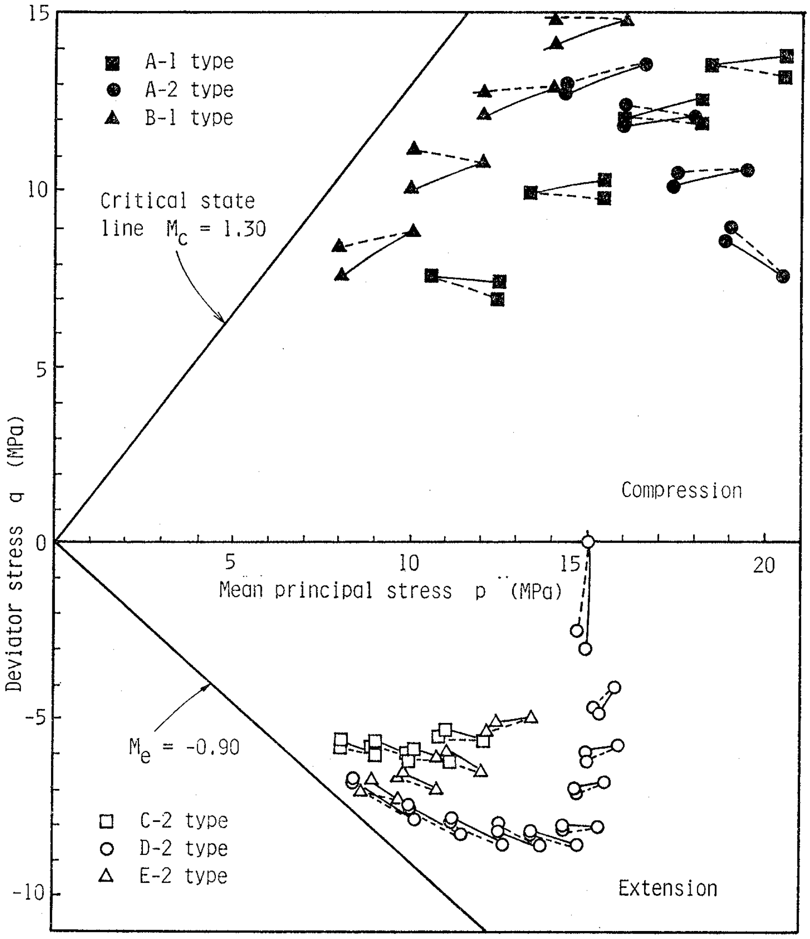

Fig. 6. Family of yield curve segments obtained by triaxial compression and extension tests

respectively, by using yield stress q_y on $q-\varepsilon$ curve, and p_y on $p-v$ curve. This method, however, brings such a few problems that the entire yield curve constructed from these yield curve segments is considerably different from the predicted yield curve, and besides that the entire yield curve does not satisfy the condition $d\varepsilon^p/dv^p=0$ at the critical state (Miura et al., 1982 b). Hence, another method for determininig the yield curve segments is examined to remove the above stated problems, and the results obtained by these two methods are compared in the following discussion.

At the associated yield points on $q-\varepsilon$ curve and $p-v$ curve, as shown in Figs. 7(a) and (b), the plastic strain increments $\delta\varepsilon^p$ and δv^p corresponding to certain stress increments δq and δp are determined, thereby we can depict a plastic strain increment vector on $p-q$ diagram, Fig. 7(c). Accepting the normality condition, we obtain the

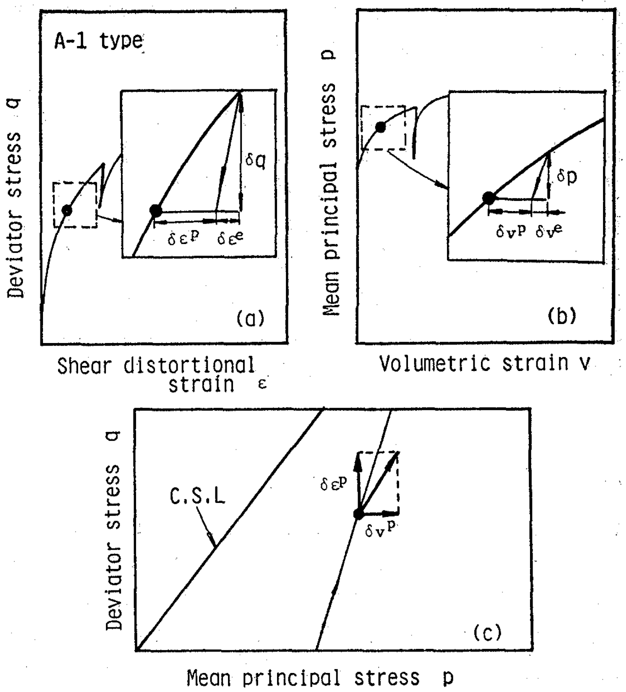

Fig. 7. Determination of plastic strain increments, (a) and (b), and plastic strain increment vector (c)

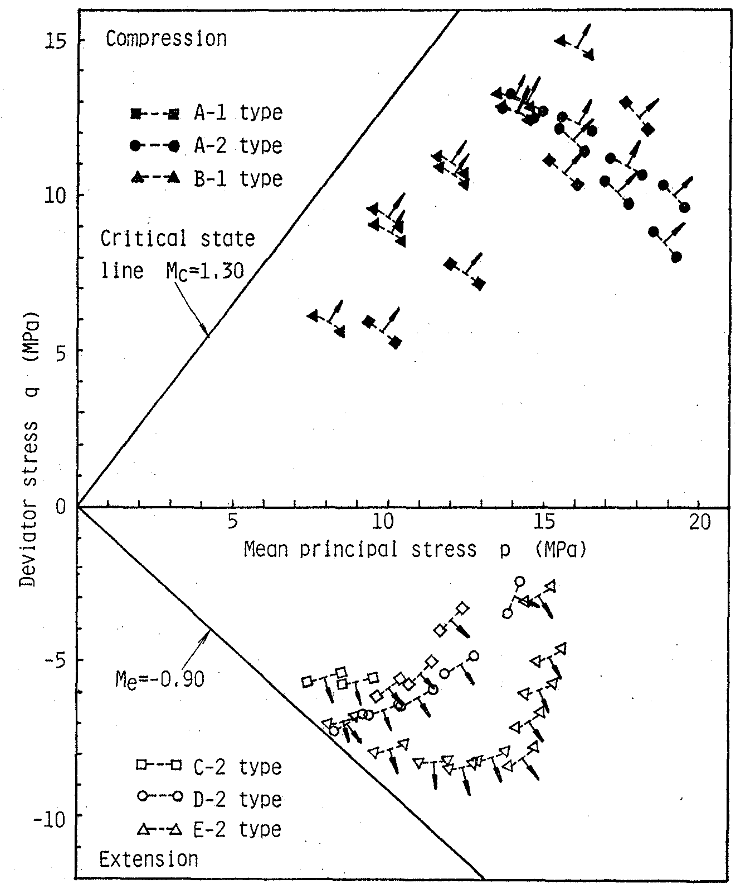

Fig. 8. Family of yield curve segments based on the normality condition

yield curve segment as a curve perpendicular to the vector as shown in Fig. 8 in broken lines.

Miura et al. (1982 b) found that the characteristics of the curve segments shown in Fig. 6 are of unique function of stress ratio η, in both compression and extension stress regions. Now, the general movement of the yield curve segments shown in Fig. 8 seem also to be a uniqe function of stress ratio, i. e, there may exist the next relationship,

$$\frac{dq}{dp}=G(\eta) \qquad (5)$$

To examine this relationship, the characteristics of the yield curve segments of the sample were investigated under the conditions both of compression and extension stresses as follows. Let the stress parameters at both ends of a yield curve segment be (p_1, q_1, η_1) and (p_y, q_y, η_y), respectively, then the values of dq/dp and η of the segment $\widehat{1Y}$ may be evaluated by the following equations:

$$\left.\begin{aligned} \frac{dq}{dp}&=(q_1-q_y)/(p_1-p_y) \\ \eta&=\frac{\eta_1+\eta_y}{2} \end{aligned}\right\} \qquad (6)$$

Fig. 9 shows the $dq/dp-\eta$ characteristics of the yield curve segments presented in Fig. 8, which suggests that Eq. (5) is applicable for cases of extension stress as well as compression stress. Then, we conclude that, within the scope of the present experiments, the yield curve of sand in a particle-crushing region depends only on the stress ratio, and not on the stress path.

Formation of the Yield Curves

Using Eq. (5) an entire yield curve can be formed as follows. From the equation $q=\eta p$, we get $dq=\eta dp+pd\eta$. Putting this relationship into Eq. (5) and integrating, we obtain,

$$\left.\begin{aligned} p&=\frac{p_i}{U_p(\eta_i)}\cdot U_p(\eta) \\ q&=\eta p \\ U_p(\eta)&=\exp\left(\int_0^\eta \frac{1}{G(\eta)-\eta}d\eta\right) \end{aligned}\right\} \qquad (7)$$

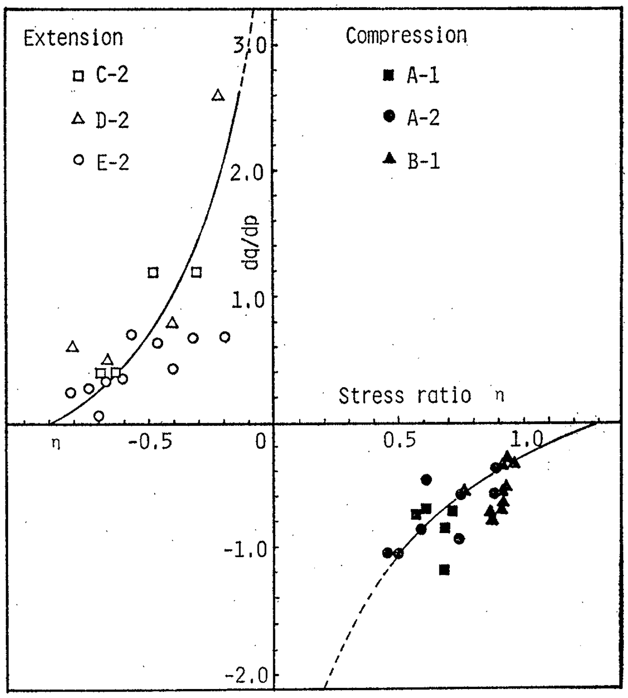

Fig. 9. ***dq/dp—η* characteristics of the yield curve segments represented in Fig. 8**

where p_i is an integrating constant, i. e., the value of p on the current yield curve at a value of η equal to η_i. Now consider a new parameter p_e defined as the value of p corresponding to η of zero. The parameter p_e is obtained from the first equation of Eq. (7), $p_{\eta=0}=p_e=(p_i/U_p(\eta_i))\cdot U_p(0)$, where $U_p(0)=1$.
Hence,

$$p_e=\frac{p_i}{U_p(\eta_i)} \qquad (8)$$

Therefore, Eq. (7) can be expressed as,

$$\left.\begin{aligned} p&=p_e\cdot U_p(\eta) \\ q&=\eta p \end{aligned}\right\} \qquad (9)$$

To depict the yield curve in the $p-q$ diagram using Eq. (7) or (9), it is necessary to use arbitrarily chosen stresses (p_i, η_i) and the $\eta-U_p(\eta)$ relationship. So far, we have no analytical equation for $\eta-U_p(\eta)$; instead, the $dq/dp-\eta$ curve was obtained by numerical integration, as shown in Fig. 10. Fig. 11 shows the yield curves depicted using Eq. (9) and $\eta-U_p(\eta)$ relationship of Fig. 10, together with the yield curve segments of Fig. 8. This figure indicates that the yield curves

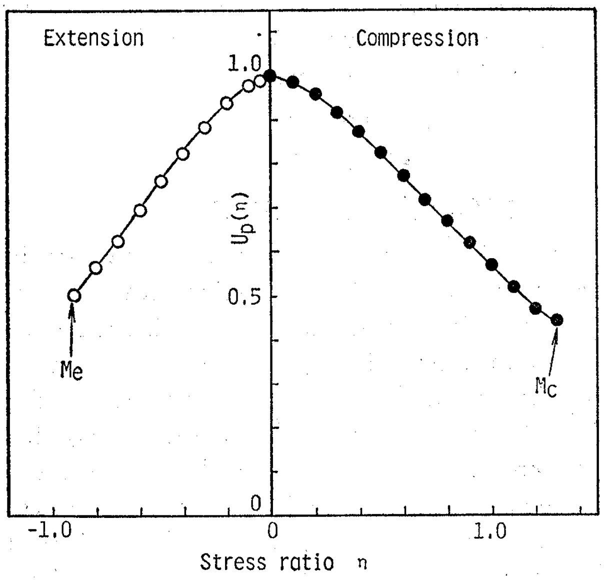

Fig. 10. $\eta - U_p(\eta)$ **curve obtained by integrating the** $dq/dp-\eta$ **curve**

based on Eq. (9) approximately agree with the yield curve segments observed.

Fig. 12 compares the yield curve I depicted by the above stated method with the yield curve II constructed by the method illustrated in Fig. 5 (detailed description of curve II appeared in Miura et al., 1982 b). It seems that the distance between the two curves becomes larger as the stress ratio η increases. As stated previously, the curve II does not satisfy the normality condition and $d\varepsilon^p/dv^p=0$ at the critical state, while the curve I satisfies both conditions. The difference between the two curves might be explained by applying an anisotropic hardening model (Mróz et al., 1981; Hashiguchi, 1983), where the yield surfaces are assumed to move in a boundary surface. In other words, the curve II may be interpretated as an elastic-plastic boundary that takes into consideration of the yield curve movement caused by unloading and reloading. However, detailed discussions on this problem requires further investigation and it is out

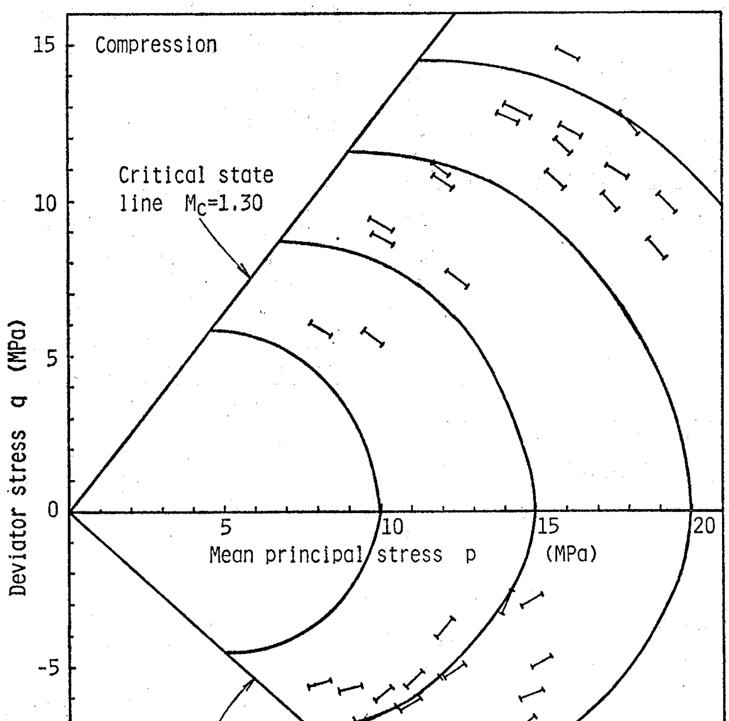

Fig. 11. Family of yield curves depicted from Fig. 10 and Eq. (9)

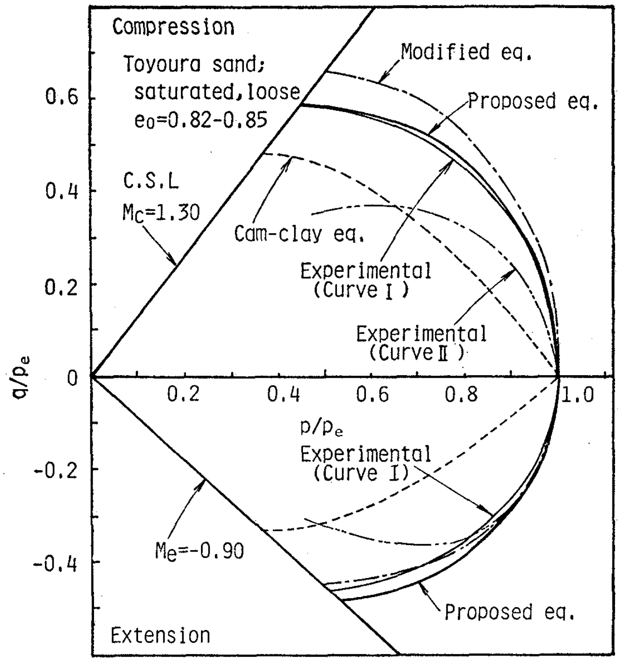

Fig. 12. Comparison of the predicted and experimental yield curves

of the scope of this study. In the following, therefore, discussions will be made only on the yield curve I.

In Fig. 12, other two yield curves are also depicted based on the Cam-clay equation and its modified equation (Roscoe and Burland, 1968). The curve I is located between the two predicted curves, suggesting that there exists a more conformable equation for predicting the yield curve of sand in a particle-crushing region.

EQUATION FOR THE YIELD CURVE

The yield curve of the Cam-clay equation and its modified equation are expressed as follows (Roscoe and Burland, 1968).

Cam-clay equation:

$$\frac{p}{p_0}=\exp\left(\frac{-\eta}{M}\right) \qquad (10)$$

Modified equation:

$$\frac{p}{p_0}=\frac{M^2}{M^2+\eta^2} \qquad (11)$$

where, p_0 is the value of p_i at η equal to zero.

The above equation was derived assuming the next expressions for the energy dissipation per unit volume, δW.

For the Cam-clay equation:

$$\delta W=pM\delta\varepsilon^p \qquad (12)$$

For the modified equation:

$$\delta W=p\sqrt{(\delta v^p)^2+(M\delta\varepsilon^p)^2} \qquad (13)$$

where, δv^p is a plastic volumetric strain increment and $\delta\varepsilon^p$, a plastic shear distortional strain increment. The difference of the yield curve Eqs. (10) and (11) depends only on the difference in the expressions for δW. On the other hand, as seen in Fig. 12, the experimental yield curve lies within the Cam-clay and the modified equation curves in compression region, and it lies without the two curves in the extension region. Therefore, in order to obtain a more conformable equation that agrees with the experimental yield curves in both compression and extension stress regions, the authors searched for a better expression for δW. The similar investigation was made by Hashiguchi (1978). After all, the authors found the following expression to give an excellent result.

$$\delta W=p\sqrt{(\delta v^p)^2+(M\delta\varepsilon^p)^2-(M\eta)^2\delta v^p\delta\varepsilon^p} \qquad (14)$$

Based on this expression the yield curve equation is derived as,

$$\frac{p}{p_0}=\exp\left[-\int_0^\eta\frac{(2+M^2\eta)\eta}{M^2\eta^3+\eta^2+M^2}d\eta\right] \qquad (15)$$

The yield curve of Eq. (15) is depicted in Fig. 12 in thick line, which is well comparable with the experimantal yield curve I. Thus, Eq. (15) proves to be reasonable for predicting the yield curve of sand in a particle-crushing region.

PREDICTION OF THE STRESS-STRAIN RELATIONSHIP

To predict the stress-strain relationship of the sand in a particle-crushing region, the applicability of the following three stress-strain equations are comparably investigated; the Cam-clay equation and the modified equation (Roscoe and Burland, 1968), and the proposed equation.

The Cam-clay equation is expressed as,

$$\left.\begin{aligned}\delta v&=\frac{1}{1+e}\left(\frac{\lambda-\kappa}{M}\delta\eta+\lambda\frac{\delta p}{p}\right)\\ \delta\varepsilon&=\frac{\lambda-\kappa}{1+e}\left[\frac{p\delta\eta+M\delta p}{Mp(M-\eta)}\right]\end{aligned}\right\}\qquad(16)$$

Burland (Roscoe and Burland, 1968) proposed the following modified equation based on the Eq. (13) for energy dissipation per unit volume,

$$\left.\begin{aligned}\delta v&=\frac{1}{1+e}\left[(\lambda-\kappa)\frac{2\eta\delta\eta}{M^2+\eta^2}+\lambda\frac{\delta p}{p}\right]\\ \delta\varepsilon&=\frac{\lambda-\kappa}{1+e}\left(\frac{2\eta}{M^2-\eta^2}\right)\left(\frac{2\eta\delta\eta}{M^2+\eta^2}+\frac{\delta p}{p}\right)\end{aligned}\right\}\qquad(17)$$

Besides the se two equations, we present a new stress-strain relationship obtained by using the Eq. (14) instead of the Burland's expression (13). The revised equation for δv and $\delta\varepsilon$ are given as,

$$\left.\begin{aligned}\delta v&=\frac{\lambda}{1+e}\left[\frac{\delta p}{p}+\left(1-\frac{\kappa}{\lambda}\right)\frac{(2+M^2\eta)\eta}{M^2\eta^3+\eta^2+M^2}\delta\eta\right]\\ \delta\varepsilon&=\frac{\lambda-\kappa}{1+e}\left[\frac{\delta p}{p}+\frac{(2+M^2\eta)\eta}{M^2\eta^3+\eta^2+M^2}\delta\eta\right]\\ &\quad\times\left[\frac{(2+M^2\eta)\eta}{M^2-\eta^2}\right]\end{aligned}\right\}\qquad(18)$$

For simplicity these equations assume that the elastic component of the shear distortional strain increment $\delta\varepsilon^e$ is negligible. Therefore, a stress change within the yield curve gives only the elastic volumetric strain v^e. When stress is applied across the present yield curve, elastic and plastic strains occur and the values of strain can be caluclated by Eqs. (16), (17) and (18).

For the standard triaxial test (constant σ_r), the stress-strain curves were predicted as shown in Fig. 13, compared with the experimental curves. In this figure, the values of

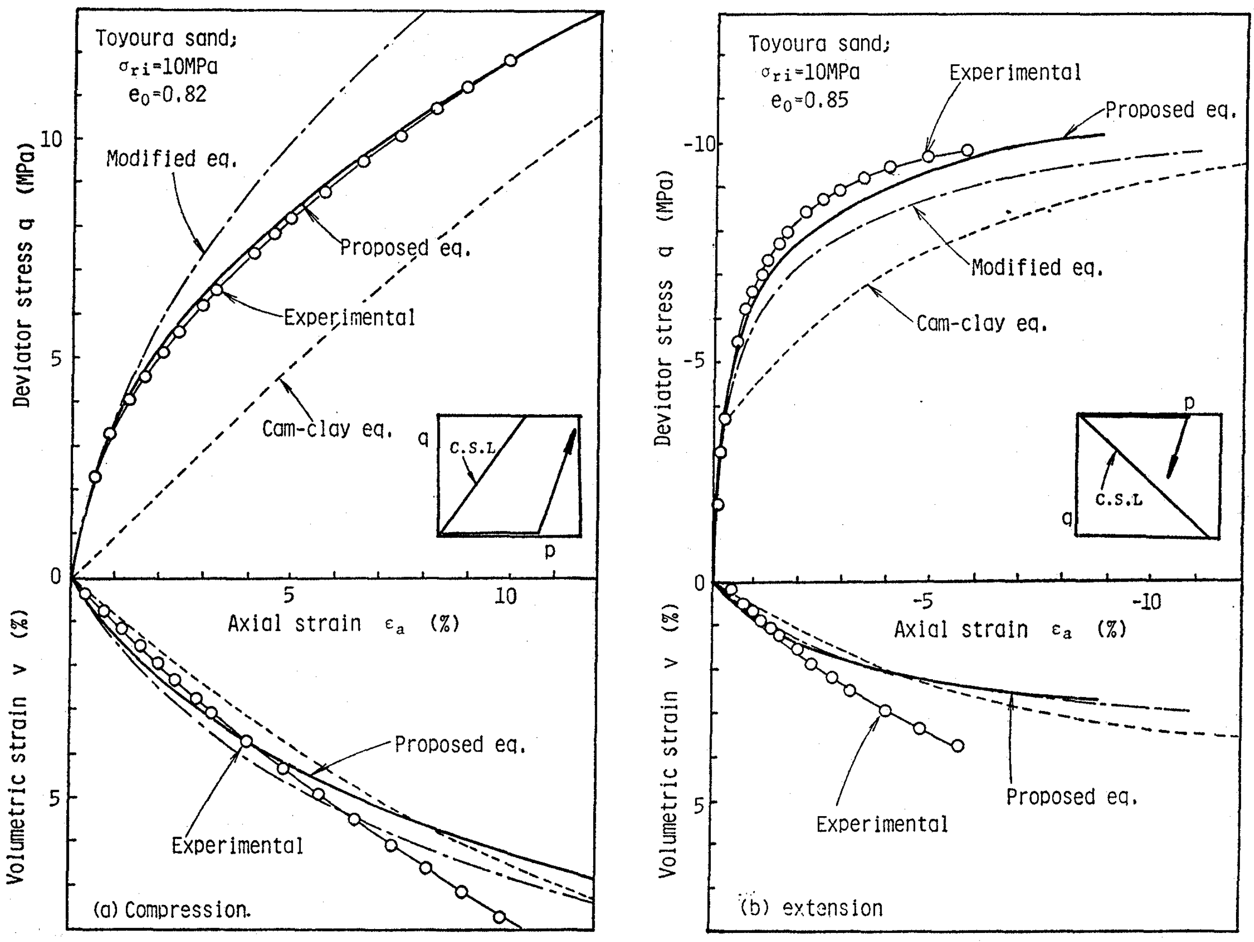

Fig. 13. Prediction of stress-strain curve for standard triaxial test (constant σ_r)

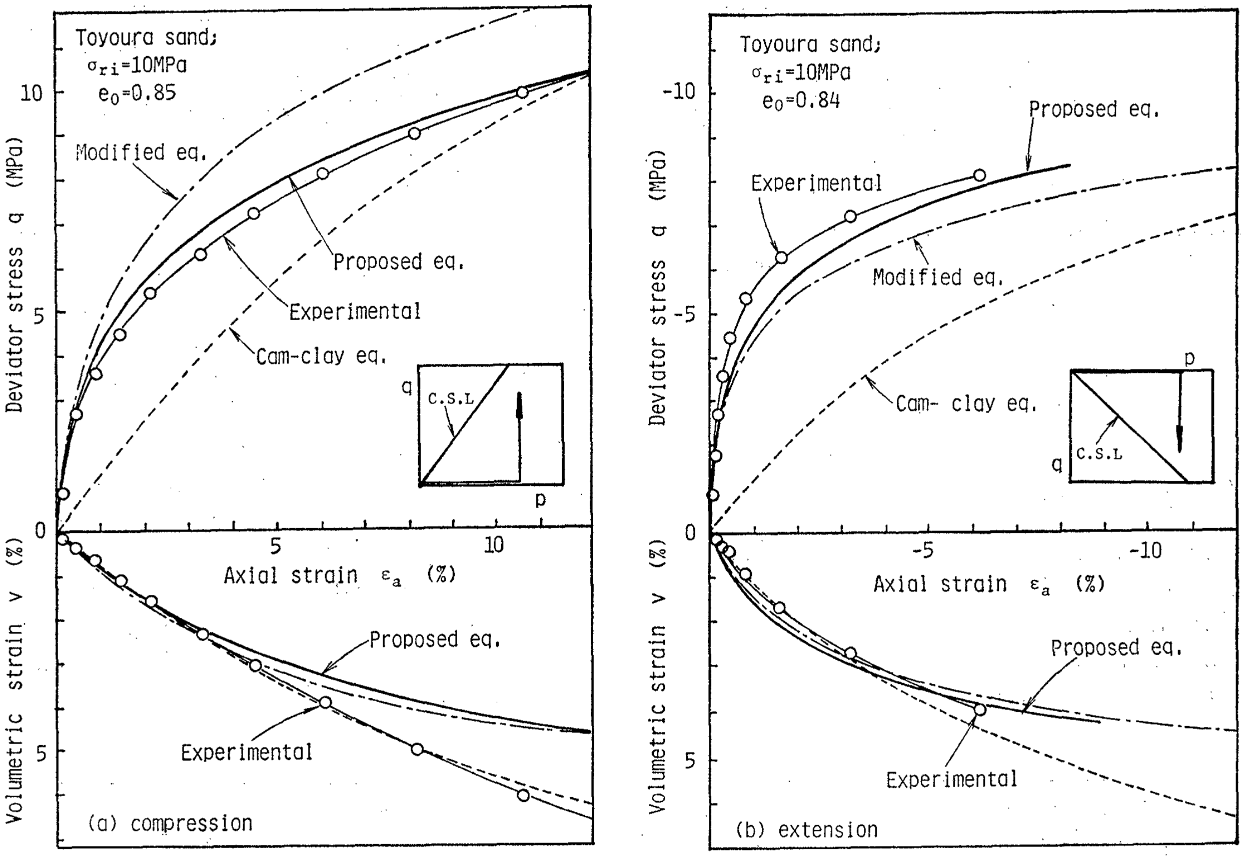

Fig. 14. Prediction of stress-strain curve for constant p triaxial test

q predicted by the three equations apparently approach to $q=Mp=1.30\,p$ at a large axial strain, hence it is sufficient to discuss within a limited axial strain of 15% for comparison of the experimental curve with the predicted curves. These results show that the Cam-clay equation tends to overestimate the axial strain in both compression and extension stress regions. On the other hand, the modified equation underestimates the axial strain in compression stress region, but overestimates in extension stress region. A similar tendency was also observed for a normally consolidated clay (Roscoe and Burland, 1968). As compared with the results predicted by the Cam-clay and the modified equations, the stress-strain curves predicted by Eq. (18) agree very well with the experimental curves, although the proposed equation still lies apart from the observed $\varepsilon_a - v$ curves.

For the drained triaxial tests at constant p, the experimental and predicted stress-strain curves are compared as shown in Fig. 14.

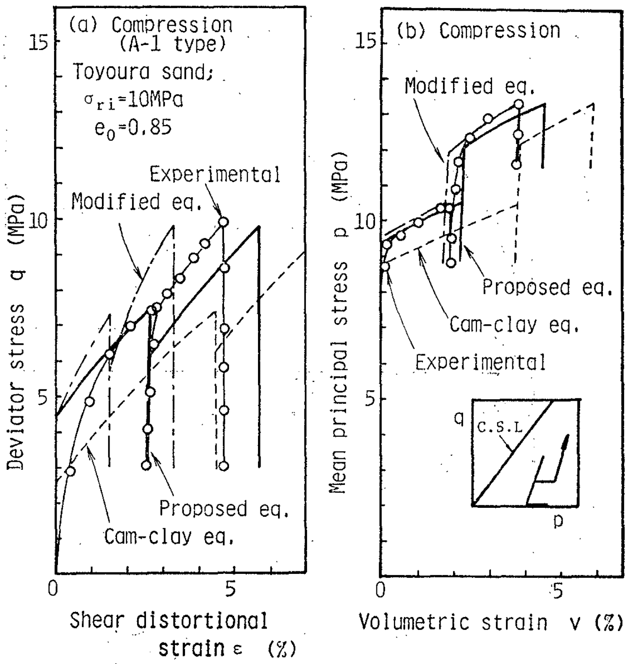

Fig. 15. Prediction of stress-strain curve in compression stress region for multi-step stress path test (A-1 type)

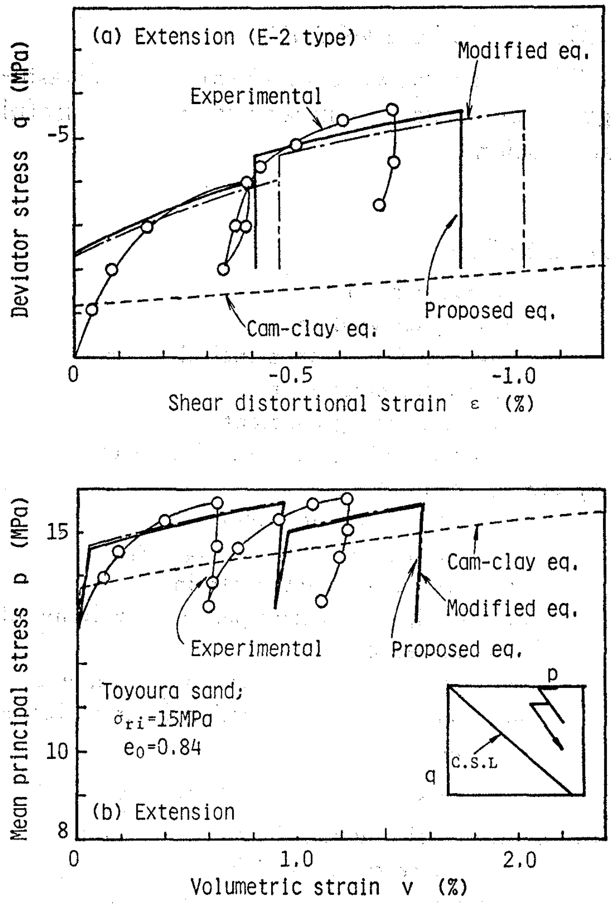

Fig. 16. Prediction of stress-strain curve in extension stress region for multi-step stress path test (E-2 type)

The result is very similar to the case of the constant σ_r triaxial tests.

Fig. 15 shows the comparisons of the experimental curve with the predicted stress-strain curves in compression stress region for the multi-step stress path test of type A-1, and Fig. 16 is the same diagram in the extension stress region for the test of type E-2. In these calculations the yield points were predicted on the basis of the Eqs. (10), (11) and (15). It is clear that these results show the similar tendency in the case of standard triaxial test. In all cases, the proposed Eq. (18) seems to predict the stress-strain relationship more accurately than do the other two equations.

The applicability of the proposed stress-strain equation for the other soils is briefly mentioned. Fig. 17 indicates the comparison of the predicted and experimental stress-strain curves for a normally consolidated kaolin tested by Walker (Roscoe and Burland, 1968), showing that the proposed equation satisfactorily predicts the experimental curves. Besides, the authors had found that the stress-strain curves of rockfill materials and a normally consolidated clay locates between the Cam-clay and the modified equation curves (Miura et al., 1977, 1980). From

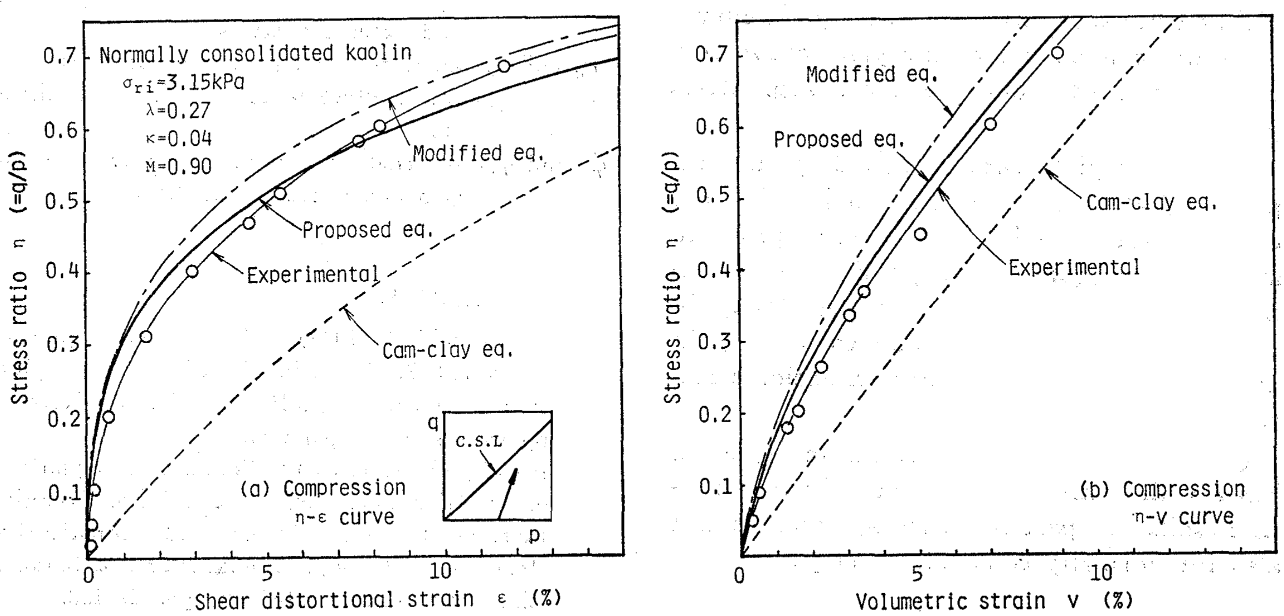

Fig. 17. Prediction of stress-strain curve of a normally consolidated kaolin tested by Walker (Roscoe and Burland, 1968)

these facts, it can be said that the proposed equation has a wide conformability not only for granular soils in particle-crushing region but also for normally consolidated clays.

CONCLUSIONS

To investigate the stress-strain characteristics of sand in a particle-crushing region, various kinds of triaxial tests including multi-step stress path tests were carried out on Toyoura sand in a saturated loose state using a high pressure triaxial apparatus. The following main conclusions were obtained.

(1) The values of the frictional constant M_c and M_e measured under compression and extension stresses were $M_c=1.30$ and $M_e=-0.90$, respectively. These values approximately satisfy the relationship $M_e=-3M_c/(3+M_c)$, derived from the Mohr-Coulomb hypothesis $\phi_e=\phi_c$.

(2) The characteristics of the yield curve which is determined on the basis of the plastic strain increment vectors under triaxial compression and extension stresses can be expressed as $dq/dp=G(\eta)$, irrespective of stress path.

(3) On the basis of the $dq/dp-\eta$ curve determined by the experiments, a family of yield curves was obtained. These yield curves are quite comparable to the yield curve segments obtained from the multi-step stress path tests.

(4) The yield curve depicted by the proposed equation is well comparable with the experimental yield curve. The proposed stress-strain equation can predict the experimental stress-strain curves satisfactorily in conditions of constant σ_r and constant p in both triaxial compression and extension stress regions.

(5) The proposed stress-strain equation has a wide conformability not only for granular soils in particle-crushing regions but also for normally consolidated clays.

ACKNOWLEDGEMENT

The authors wish to thank Dr. K. Hashiguchi at Kyushu University for his useful suggestion.

NOTATION

e = void ratio
e_0 = initial void ratio
p = effective mean principal stress
p_e = stress parameter
p_i = integrating constant
p_0 = value of p_i at η equal to zero
p_y and q_y = yield stresses
q = axial deviator stress
v = volumetric strain $(=\varepsilon_a+2\varepsilon_r)$
v^e = elastic volumetric strain
δW = dissipated energy per unit volume of material
δv^p = plastic volumetric strain-increment
$\delta\varepsilon^p$ = plastic shear distortional strain-increment
ε = shear distortional strain $\left(=\frac{2}{3}(\varepsilon_a-\varepsilon_r)\right)$
ε_a and ε_r = axial and radial principal strains
η = stress ratio $(=q/p)$
η_{cs} = stress ratio at the critical state
κ = slope of swelling line of e-$\log p$ curve
λ = slope of normally consolidation line of $e-\log p$ curve
M = frictional constant at the critical state
M_c and M_e = frictional constants under compression and extension stresses
σ_a and σ_r = axial and radial effective stresses
σ_{ri} = radial effective stress after consolidation
ϕ_c and ϕ_e = internal friction angles under compression and extension stresses

REFERENCES

1) Hashiguchi, K. (1978) : "Constitutive equation of soils : 7. Theories based on elastoplasticity," Jour. of JSSMFE, Vol. 18, No. 4, pp. 131-142 (in Japanese).
2) Hashiguchi, K. (1983) : "Constitutive equations of granular materials," Mechanics of Granular Materials : New Models and Constitutive Relations, Ed. by J. T. Jenkins and M. Satake, Elsevier Science Publishers, pp. 127-136.
3) Kondner, R. L. and Zelasko, J. S. (1963) : "Void ratio effects on the hyperbolic stress-

strain response of a sand," Laboratory Shear Testing of Soils, ASTM, STP No. 361, pp. 250-257.

4) Miura, N., Noriyasu, N. and Ayaghi, K. (1977) : "Stress-strain characteristics of a loose sand under high pressure," Memoirs of the Yamaguchi Univ., Vol. 27, No. 2, pp. 215-223 (in Japanese).

5) Miura, N. and Yamanouchi, T. (1977) : "The effect of the particle-crushing on the shear characteristics of a sand," Proc. JSCE, No. 260, pp. 109-118 (in Japanese).

6) Miura, N. (1979) : "A consideration on the stress strain relationship of a sand under high pressures," Proc. JSCE, No. 282, pp. 127-130 (in Japanese).

7) Miura, N. and Yamamoto, N. (1980) : "A consideration on the stress strain characteristics of rockfill materials," Memoirs of the Yamaguchi Univ., Vol. 30, No. 2, pp. 233-240 (in Japanese).

8) Miura, N. and Yamamoto, N. (1982 a) : "On the yield curve of sand in particle-crushing regions," Proc. JSCE, No. 326 pp. 83-90 (in Japanese).

9) Miura, N. and Yasufuku, N. (1982 b) : "Yielding characteristics of sand under triaxial compression and extension stresses," Tech. Reps. of the Yamaguchi Univ., Vol. 3, No. 1, pp. 33-45.

10) Mróz, Z., Norris, V. A. and Zienkiewicz, O. C. (1981) : "An anisotropic, critical state model for soils subject to cyclic loading," Géotechnique, Vol. 31, No. 4, pp. 451-469.

11) Poorooshabs, H. B., Holbec, I. and Sherbourne, A. N. (1967) : "Yielding and flow of sand in triaxial compression, Part II and III," Canadian Geotechnical Journal, Vol. 4, pp. 377-398.

12) Roscoe, K. H. and Burland, J. B. (1968) : "On the generalized stress strain behavior of "wet" clay," Engineering Plasticity, Cambridge Univ. Press., pp. 535-609.

13) Schofield, A. and Wroth, P. (1968) : Critical State Soil Mechanics, McGraw-Hill Book Company, New York.

14) Tatsuoka, F. and Ishihara, K. (1974) : "Yielding of sand in triaxial compression," Soils and Foundations, Vol. 14, No. 2, pp. 63-76.